RADIO TRANSIENT DETECTION IN RADIO ASTRONOMICAL ARRAYS

Avishay Antman

Faculty of Engineering, Bar-Ilan University
Ramat-Gan 52900, Israel

Amir Leshem

Faculty of Engineering, Bar-Ilan University
Ramat-Gan 52900, Israel

ABSTRACT

Celestial transient radio sources have attracted considerable scientific interest recently, but their investigation is hampered by the fact that they cannot be effectively detected by commonly used radio astronomy imaging techniques. One significant obstacle to observing radio transients is intermittent terrestrial radio frequency interference, which can appear as a transient signal. In this paper we propose two schemes for the detection of transient sources. The first is a generalized likelihood ratio test designed for terrestrial interferences that appear in the near field region. The second is a modification of the first one, designed for sources whose steering vector is known to be in the array manifold, such as astronomical sources. Both of the proposed detectors are based on two consecutive sample covariance matrices computed by the array, and they have the desirable property of a constant false alarm rate. We provide a simple analysis of the proposed method as well as a computer simulation. The computer simulation results suggest that the proposed detectors outperform the detector that is currently used by the low frequency array (LOFAR) radio telescope processor.

1. INTRODUCTION

A short duration, non-periodical celestial radio signal was detected for the first time in 2007 [17], and fewer than 20 other such fast radio bursts (FRB) have been detected since then [19]. The study of FRBs and their origin is of great scientific interest because they are considered to be a product of exotic astronomical events. It is likely that only a small fraction of FRBs incident on Earth are detected, since current radio telescopes and imaging methods are not adapted for a large field of view, a high sensitivity to transients, or full time coverage. Enormous efforts are being made to develop new telescopes, processing hardware and algorithms that will provide better temporal, spatial and frequency coverage for the detection and accurate analysis of transient astronomical signals [18].

Similarly to the detectors in [15] and [16], the detectors developed in this work are also applicable to cognitive radio, passive radar, passive acoustic sensors and any other multi-sensor receiving system that can benefit from detecting short duration, spatially localized Gaussian signals that are embedded in colored Gaussian noise.

The sensor (specifically, a radio telescope designed for the search of astronomical transients) is assumed to generate a sequence of sample covariance matrices (SCM), where each SCM corresponds to a distinct set of vector samples collected during a time frame of constant length [20] [21]. The SCM integration interval is short enough so that the statistical properties of all the received signals, except for transients, can be assumed to remain constant during two consecutive time frames. The signal of interest is expected to be a Gaussian point source that appears and disappears during one integration interval. We further assume that all the signals, both static and transient, are zero-mean Gaussian, and that the occurrence of transients is rare, so that there may be at most one transient point source in a single SCM. The work presented here focuses on detecting a spatially correlated Gaussian signal using a given pair of consecutive SCMs. The problem of detecting spatially correlated signals using one or more SCMs has been addressed in works for various statistical signal and noise models. In [14] and [15] it is assumed that the noise is spatially uncorrelated, or that its spatial covariance is very small compared to the covariance of the desired signal. In [13] and [3] generalized likelihood ratio test (GLRT) detectors are developed for the detection of an unknown deterministic signals that are restricted to some given subspace, and embedded in spatially correlated Gaussian noise. In [13] the noise covariance matrix is assumed to be known up to some scaling factor and in [3] the availability of a secondary dataset that contains only background signal is assumed, which is similar to the settings of our work. The difference lies in the signal model taken — whereas Bandiera et al. assumed a deterministic, unknown signal whose steering vector (SV) is bound to a given subspace, we assume a Gaussian signal that may appear anywhere in $\mathbb{C}^q$, where q denotes the number of antennas in the array (or in some array manifold whose elements span $\mathbb{C}^q$).

We consider the problem of transient detection for two types of signal models that differ in terms of the prior knowledge about the set in which the transient SV is expected to be. In the structured SV model, it is assumed that the transient SV is restricted to the array manifold. The detector developed for this model is adequate for the detection of far field transient radio sources. The unstructured SV assumes no knowledge about the source SV. The detector developed for this model is appropriate for cases where the array is not calibrated or the transient signal originates from the near field region of the array (which may span a very large area for a radio telescope with long baselines).

The detectors developed for both signal models use the maximum value of a real function known as the "pixel likelihood function" as the test statistic. In the unstructured case, this maximal value can be reduced to the largest joint eigenvalue of two random Wishart matrices. The asymptotic distribution of this largest joint eigenvalue as given in [11] for H_0, together with the results of [10] [8] [1] can be used for the theoretical analysis of the detectors' performance when the input dataset is large and when both the dataset and the number of elements in the array are large.

2. PROBLEM FORMULATION

An array of q antennas receives two consecutive sample sets, each of which consists of N i.i.d. q-dimensional zero-mean complex normal vectors, that will be denoted by $\{\mathbf{r}_{j,i}\}_{i=1}^{N}$, $j = 1, 2$. The covariance of the vectors of the first set will be referred to as the background

This work was supported by ISF grants 903/2013 and 1240/2009

covariance matrix (BCM) and denoted by R_*, and the covariance of the vectors of the second set depends on the true hypothesis. Under H_0 it is the same as the covariance matrix of the first set, i.e. R_*, and under H_1 which states that a transient source with SV $\mathbf{a}_*$ and power σ_*^2, appeared during the second interval, a rank-1 Hermitian matrix of the form $\sigma_*^2 \mathbf{a}_* \mathbf{a}_*^H$ is appended to the BCM, so that the distribution of the samples under both hypotheses can be written as follows

$$\mathbf{r}_{1,i} \sim CN(0, R_*),\ i = 1, ..., N \tag{1}$$

$$\mathbf{r}_{2,i} \sim \begin{cases} CN(0, R_*) & H_0 \\ CN(0, Q(R_*, \mathbf{a}_*, \sigma_*^2)) & H_1 \end{cases},\ i = 1, ..., N \tag{2}$$

where $CN(\mu, \Sigma)$ denotes the proper complex vector Gaussian distribution with mean μ and covariance Σ, and

$$Q(R, \mathbf{a}, \sigma^2) \equiv R + \sigma^2 \mathbf{a}\mathbf{a}^H \tag{3}$$

Because under both hypotheses, each set of measurements $\{\mathbf{r}_{1,i}\}$ and $\{\mathbf{r}_{2,i}\}$ is modeled as a set of i.i.d. zero-mean complex Gaussian vectors, the two SCMs $\hat{R}_1$ and $\hat{R}_2$ defined as

$$\hat{R}_k = \frac{1}{N} \sum_{i=1}^{N} \mathbf{r}_{i,k} \mathbf{r}_{i,k}^H,\ k = 1, 2 \tag{4}$$

are a sufficient statistic for estimating the unknown parameters, and therefore contain all the information that can be used when deriving the estimators and the test statistic. The observation set $\mathbf{Y}$ input to the detector is represented as an ordered pair of the SCMs

$$\mathbf{Y} \equiv (\hat{R}_2, \hat{R}_1) \in \mathbf{S}_+^q \times \mathbf{S}_+^q \tag{5}$$

where $\mathbf{S}_+^q$ denotes the set of $q \times q$ positive definite (PD) matrices.

The probabilities of detection and false alarm are given by $P_d = \Pr(\hat{H}(\mathbf{Y}) = H_1 | H_1, \theta_1)$ and $P_{fa} = \Pr(\hat{H}(\mathbf{Y}) = H_1 | H_0, \theta_0)$ respectively, where $\hat{H}(\mathbf{Y}) \in \{H_0, H_1\}$ denotes the decision of a detector as a function of the measurements and $\Pr(A | H_i, \theta_i),\ i \in \{0, 1\}$ denotes the probability of A when the true hypothesis is H_i with a corresponding set of parameters θ_i which will be detailed in subsection 4.1.

We assume without loss of generality that

$$\hat{R}_1 - \hat{R}_2 \notin \mathbf{S}_+^q \tag{6}$$

which implies that a vector $\mathbf{x}$ may always be found such that $\mathbf{x}^H (\hat{R}_2 - \hat{R}_1) \mathbf{x} \geq 0$, since otherwise, the energy received from any direction during the second sampling interval is lower than what was received during the first interval and any reasonable detector will decide H_0 ("no transient signal") in that case.

2.1. Structured and unstructured problem settings

We consider two different problem settings: the "structured SV" and "unstructured SV" models. In the structured model it is assumed that the transient source is located in the far field region of the array and that the array manifold, denoted by S, is known and contained in the unit sphere of $\mathbb{C}^q$, denoted by $C^q \equiv \{\mathbf{x} \in \mathbb{C}^q, \|\mathbf{x}\|_2 = 1\}$.

In the unstructured model no prior knowledge about $\mathbf{a}_*$ is assumed and the search domain is C^q. The derivation of the detectors will be done separately for each of the cases.

A practical detection scheme may use these two detectors sequentially. In the first detection stage, the unstructured detector is applied with a low threshold level (for high probability of detection (P_d) and a high false alarm rate (FAR)) in order to detect any suspicious signal, and then uses the SV estimation to only pass celestial signals to the next stage. In the second stage, the structured detector, which outperforms the unstructured detector for celestial sources, is used to confirm or reject the first stage detections. This way, terrestrial interferences are filtered out from the detection process, and the computation demands are relaxed compared to a detection scheme that passes all the data to the structured detector.

3. OVERVIEW OF EXISTING DETECTORS

3.1. The clairvoyant detectors

The detectors that will be presented next are unrealizable since they require information that is not available; hence they will be only used as upper bounds and points of reference for the achievable performance of the GLRT based detector, and to better understand its properties.

Suppose we had prior knowledge that under H_1 the transient SV would be $\mathbf{a}_*$ and that under both H_0 and H_1 the true BCM is R_*. A uniformly most powerful (UMP) [12] test statistic for this detection problem would be

$$T_{\mathbf{a}_*}(\mathbf{Y}) = m(\mathbf{a}_*, R_*, \hat{R}_2) \tag{7}$$

where the function $m(\mathbf{x}, A, B) : (\mathbb{C}^q \times \mathbf{S}_+^q \times \mathbf{S}_+^q) \to \mathbb{R}$, defined as

$$m(\mathbf{x}, A, B) \equiv \frac{\mathbf{x}^H A^{-1} B A^{-1} \mathbf{x}}{\mathbf{x}^H A^{-1} \mathbf{x}} \geq 0 \tag{8}$$

will be referred to as the "pixel-likelihood value".

An appealing feature of this statistic is that under H_0 its distribution depends solely on N.

If the BCM were known but not the transient SV, we would use (27) or (30) depending on the signal model, and replace $\hat{R}_1$ with R_* in the input arguments of $m(\cdot, \cdot, \cdot)$, leading to the simple largest eigenvalue detector for the unstructured model.

3.2. Dirty image subtraction detector

The transient detection algorithm currently used in the LOFAR processing pipeline [20] [22] takes three consecutive SCMs $\{\hat{R}_i,\ i = 1, 2, 3\}$ and detects transients in the middle one (i.e. $\hat{R}_2$) using the following test statistic

$$T_{\mathrm{DI}}(\hat{R}_1, \hat{R}_2, \hat{R}_3) = \max_{\mathbf{a} \in S} \mathbf{a}^H \left(\hat{R}_2 - \frac{1}{2}(\hat{R}_1 + \hat{R}_3) \right) \mathbf{a} \tag{9}$$

This is practically a pixel-wise second order differentiator applied to the sequence of dirty images (DI) synthesized from the sequence of SCMs. The actual processing pipeline of LOFAR is more complicated than the simple detection formula that was presented here, but the other processing stages that were omitted are not related to the topic of this paper.

4. GLRT DETECTOR FOR THE UNSTRUCTURED MODEL

For the unstructured SV problem, closed form expressions are derived for the maximum likelihood (ML) estimators of the unknown parameters under H_0 and H_1, for the maximal log-likelihood values and for the corresponding GLRT statistic. A brief outline of the derivation and the final results will be given in following subsections.

4.1. The log-likelihood functions

To derive the GLRT in the unstructured case, we first compute the log-likelihood functions under each hypothesis. Under H_0 all the observations are drawn independently from the same distribution; with the only unknown parameter being the BCM $\theta_0 = \{R\}$, the log-likelihood of a given set $\mathbf{Y}$ as a function of the BCM $R \in \mathbf{S}_+^q$ is

$$\log p(\mathbf{Y}; H_0, R) = -2N\left(q \log \pi + \log |R| + \text{tr}\left(R^{-1}\hat{M}\right)\right) \tag{10}$$

where $|\cdot|$ and tr$(\cdot)$ denote the determinant and trace operators, and

$$\hat{M} \equiv \frac{1}{2N}\sum_{k=1}^{2}\sum_{i=1}^{N}\mathbf{r}_{i,k}\mathbf{r}_{i,k}^H = \frac{1}{2}\left(\hat{R}_1 + \hat{R}_2\right) \tag{11}$$

Under H_1, the set of 3 unknown parameters is $\theta_1 \equiv \left\{R, \mathbf{a}, \sigma^2\right\}$ and the log-likelihood of $\mathbf{Y}$ as a function of θ_1 is

$$\begin{aligned}\log p(\mathbf{Y}; H_1, \theta_1) = -N\Big(&2q\log\pi + \log|R| + \log|Q(R,\mathbf{a},\sigma^2)| \\ &+ \text{tr}\left(R^{-1}\hat{R}_1 + Q(R,\mathbf{a},\sigma^2)^{-1}\hat{R}_2\right)\Big)\end{aligned} \tag{12}$$

4.2. Parameter estimation under H_0

The matrix R that maximizes (10) for a given observation set $\mathbf{Y}$ is $\hat{M}$ (as proved in [2]). The maximum log-likelihood obtained by substituting $\hat{M} \to R$ in (10) is (omitting a constant term)

$$\log p_*(\mathbf{Y}; H_0) \equiv \max_{R\in\mathbf{S}_+^q} \log p(\mathbf{Y}; H_0, R) = -2N \log|\hat{M}| \tag{13}$$

4.3. Parameter estimation under H_1

For the derivation of the ML estimator of $\hat{\theta}_1$, we need to maximize (12) with respect to 3 parameters of which σ^2 is a scalar, $\mathbf{a}$ is a q-dimensional vector and $R \in \mathbf{S}_+^q$. This maximization problem will be solved successively. We first estimate σ^2 given $\mathbf{a}$ and R. Then we estimate $\mathbf{a}$ given the ML estimate of σ^2 for each R. Finally we estimate R given the conditional estimates of $\mathbf{a}$ and σ^2:

$$\hat{\sigma}^2(\mathbf{Y}; R, \mathbf{a}) \equiv \arg\max_{\sigma^2\geq 0} p(\mathbf{Y}; R, \mathbf{a}, \sigma^2) \tag{14}$$

$$\hat{\mathbf{a}}(\mathbf{Y}; R) \equiv \arg\max_{\mathbf{a}\in C^q} p(\mathbf{Y}; R, \mathbf{a}, \hat{\sigma}^2(\mathbf{Y}; R, \mathbf{a})) \tag{15}$$

$$\hat{R}(\mathbf{Y}) \equiv \arg\max_{R\in\mathbf{S}_+^q} p\left(\mathbf{Y}; R, \hat{\mathbf{a}}(R), \hat{\sigma}^2(R, \hat{\mathbf{a}}(R))\right) \tag{16}$$

Next, we present the power estimator. Solving (14) (assuming that $\mathbf{a} \in C^q$) yields a ML power estimator that depends on the BCM and SV estimators

$$\hat{\sigma^2}(\mathbf{Y}; R, \mathbf{a}) = \left(\mathbf{a}^H R^{-1}\mathbf{a}\right)^{-1}\left(m(\mathbf{a}, R, \hat{R}_2) - 1\right)^+ \tag{17}$$

where $(x)^+ \equiv \max\{0, x\}$ and $m(\cdot,\cdot,\cdot)$ is defined in (8).

Plugging this result back into (12), we obtain the log-likelihood under H_1 as a function of 2 parameters - the BCM and the SV (omitting the same constant that was omitted in (13) and denoting $\beta(R, \mathbf{Y}) \equiv 2N(\log|R| + \text{tr}(R^{-1}\hat{M}))$)

$$\log p(\mathbf{Y}; H_1, R, \mathbf{a}) = -\beta(R, \mathbf{Y}) + Nh\left(m(\mathbf{a}, R, \hat{R}_2)\right) \tag{18}$$

where the function $h : (0, \infty) \to (-\infty, 0]$ is defined as

$$h(x) = -\left(-\log x + x - 1\right)^+ \tag{19}$$

This is a continuously differentiable decreasing function over $\mathbb{R}$.

Maximizing (18) w.r.t. $\mathbf{a}$ gives the SV dependent estimator

$$\hat{\mathbf{a}}(\mathbf{Y}; R) = \arg\max_{\mathbf{a}\in C^q} m(\mathbf{a}, R, \hat{R}_2) \tag{20}$$

which can be identified as the generalized eigenvector of the matrix pair $\mathbf{W} = (R^{-1}, \hat{R}_2^{-1})$ that corresponds to the largest joint eigenvalue of this pair, which will be denoted by $\lambda_{\mathbf{W},\max}$.

Maximizing the log-likelihood w.r.t. the power and SV yields

$$\log p(\mathbf{Y}; H_1, R) = -\beta(R, \mathbf{Y}) + Nh\left(\lambda_{\mathbf{W},\max}\right) \tag{21}$$

Maximizing (21) w.r.t. R gives the BCM ML estimator

$$\hat{R}(\mathbf{Y}) = \arg\max_{R\in\mathbf{S}_+^q} p(\mathbf{Y}; H_1, R) = \hat{M} - \frac{\lambda_{\mathbf{Y},1} - 1}{2}\mathbf{v}_{\mathbf{Y},1}\mathbf{v}_{\mathbf{Y},1}^H \tag{22}$$

where $\lambda_{\mathbf{Y},1}$ is the largest eigenvalue of the pair $\mathbf{Y} = (\hat{R}_2, \hat{R}_1)$ (defined in (5)) and $\mathbf{v}_{\mathbf{Y},1}$ is defined by

$$\hat{R}_1^{-1}\mathbf{v}_{\mathbf{Y},1} = \lambda_{\mathbf{Y},1}\hat{R}_2^{-1}\mathbf{v}_{\mathbf{Y},1}\,, \quad \mathbf{v}_{\mathbf{Y},1}^H\hat{R}_1^{-1}\mathbf{v}_{\mathbf{Y},1} = 1 \tag{23}$$

Plugging (22) into (20) we obtain the SV ML estimator that depends only on the observations

$$\hat{\mathbf{a}}(\mathbf{Y}) = \hat{\mathbf{a}}(\mathbf{Y}; \hat{R}(\mathbf{Y})) = \|\mathbf{v}_{\mathbf{Y},1}\|^{-1}\mathbf{v}_{\mathbf{Y},1} \tag{24}$$

and by plugging (22) and (24) into (17), and using the normalization given in (23), we obtain the power estimator

$$\hat{\sigma^2}(\mathbf{Y}) = \|\mathbf{v}_{\mathbf{Y},1}\|^2(\lambda_{\mathbf{Y},1} - 1) = \frac{\lambda_{\mathbf{Y},1} - 1}{\hat{\mathbf{a}}(\mathbf{Y})^H\hat{R}_1^{-1}\hat{\mathbf{a}}(\mathbf{Y})} \tag{25}$$

where we use the inequality $\lambda_{\mathbf{Y},1} \geq 1$ that follows from (6), to omit the $(\cdot)^+$ operator.

The maximal log-likelihood under H_1 is obtained by plugging the BCM estimator (22) into (21)

$$\log p_*(\mathbf{Y}; H_1) = 2N\left(\log\frac{1}{2}\left(\lambda_{\mathbf{Y},1}^{-\frac{1}{2}} + \lambda_{\mathbf{Y},1}^{\frac{1}{2}}\right) - \log|\hat{M}|\right) \tag{26}$$

The unstructured GLRT statistic

The GLRT statistic for the case of the unstructured SV is obtained by subtracting the maximal log-likelihood under H_0, given in (13) from the maximal log-likelihood under H_1 (26)

$$T_{\text{us}}(\mathbf{Y}) = 2N\log\frac{1}{2}\left(\lambda_{\mathbf{Y},1}^{-\frac{1}{2}} + \lambda_{\mathbf{Y},1}^{\frac{1}{2}}\right) \tag{27}$$

Since $\lambda_{\mathbf{Y},1} \geq 1$ and this function is monotonic for $\lambda_{\mathbf{Y},1} \geq 1$, an equivalent test statistic to $T_{\text{us}}(\mathbf{Y})$ would be

$$T'_{\text{us}}(\mathbf{Y}) = \lambda_{\mathbf{Y},1} = \max_{\mathbf{a}\in C^q} m(\mathbf{a}, \hat{R}_1, \hat{R}_2) \tag{28}$$

Using this test statistic, the GLRT detector can decide whether a transient appeared during the second time interval by computing the largest joint eigenvalue of the given SCM pair and comparing it to a constant chosen to provide a desired false-alarm rate.

The computation of the largest joint eigenvalue in (28) can be performed by applying one of the procedures described in [7] to the

composite matrix $L^{-1}\hat{R}_2 L^{-H}$, where L is the cholesky decomposition of $\hat{R}_1$ [5].

It can be shown that under H_0, the distribution of $m(\mathbf{x}, \hat{R}_1, \hat{R}_2)$ is invariant to $\mathbf{x}$ and R_*, and under H_1 its distribution depends on $\mathbf{x}$ and on the signal-background-ratio (SBR), which is defined by

$$\bar{\sigma}_*^2 \equiv \sigma_*^2 \mathbf{a}_*^H R_*^{-1} \mathbf{a}_* \tag{29}$$

5. EXTENSIONS TO THE STRUCTURED MODEL

The detection algorithm for the unstructured model assigns a pixel likelihood value given by $m(\mathbf{a}, \hat{R}_1, \hat{R}_2)$ to every SV $\mathbf{a} \in C^q$, and makes its decision based on whether the maximum pixel likelihood value crossed some threshold or not.

A natural extension of this detection algorithm to the structured SV model would result in a detector that takes the maximum pixel-likelihood among S instead of C^q. The new test statistic would be

$$T_S(\mathbf{Y}) = \max_{\mathbf{a} \in S} m(\mathbf{a}, \hat{R}_1, \hat{R}_2) \tag{30}$$

A alternative extension of the GLRT test statistic for the structured model is based on the generalized Rayleigh quotient [9] of $(\hat{R}_1^{-1}, \hat{R}_2^{-1})$, defined as the following function of $\mathbf{a}$

$$r(\mathbf{a}, \hat{R}_1, \hat{R}_2) \equiv \frac{\mathbf{a}^H \hat{R}_1^{-1} \mathbf{a}}{\mathbf{a}^H \hat{R}_2^{-1} \mathbf{a}} \tag{31}$$

Observing that $\max_{\mathbf{a}} r(\mathbf{a}, \hat{R}_1, \hat{R}_2) = \lambda_{\mathbf{Y},1}$, and that the maximizing vector in the noiseless case ($N \to \infty$) is $\mathbf{a}_*$, we introduce the following test statistic for the structured model

$$T_{\text{MVDR}}(\mathbf{Y}) = \max_{\mathbf{a} \in S} r(\mathbf{a}, \hat{R}_1, \hat{R}_2) \tag{32}$$

which is the maximal pixel-wise ratio between the MVDR image [4] synthesized from $\hat{R}_2$ and the MVDR of $\hat{R}_1$; hence, it will be referred to as the MVDR detector, and $r(\hat{R}_1, \hat{R}_2, \mathbf{a})$ as the MVDR ratio. As will be shown in section 6, the maximum pixel-likelihood and MVDR detectors perform almost identically.

Under H_0 the distributions of all 3 test statistics: $T'_{\text{us}}(\mathbf{Y})$, $T_S(\mathbf{Y})$ and $T_{\text{MVDR}}(\mathbf{Y})$ depend solely on the receiving array parameters N and q. Hence, the proposed detectors with a fixed threshold possess the constant false alarm rate (CFAR) property. Under H_1, for given N and q, the SBR is a sufficient statistic for all three.

5.1. Asymptotic distributions

For large datasets ($N \to \infty$) the statistics of both the pixel likelihood (8) and the MVDR ratio (31) functions can be approximated by the following univariate normal distributions

$$H_0: \quad \left\{ \begin{matrix} m(\mathbf{a}, \hat{R}_1, \hat{R}_2) \\ r(\mathbf{a}, \hat{R}_1, \hat{R}_2) \end{matrix} \right\} \overset{a}{\sim} N\left(1, \frac{2}{N}\right) \tag{33}$$

$$H_1: \quad \left\{ \begin{matrix} m(\mathbf{a}_*, \hat{R}_1, \hat{R}_2) \\ r(\mathbf{a}_*, \hat{R}_1, \hat{R}_2) \end{matrix} \right\} \overset{a}{\sim} N\left(\bar{\sigma}_*^2 + 1, \frac{2(\bar{\sigma}_*^2 + 1)^2}{N}\right) \tag{34}$$

where $\overset{a}{\sim}$ denotes asymptotic distribution. The proof of these asymptotic distributions is complicated and will be provided in the full version of this paper.

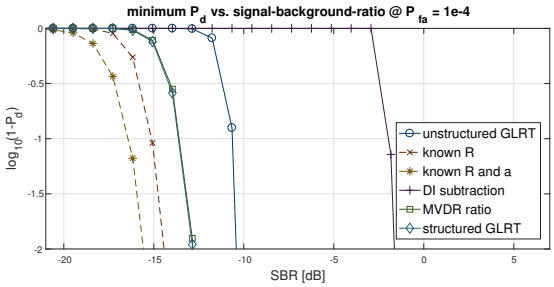

Fig. 1. simulation results

6. SIMULATION RESULTS

We first outline the simulation scheme. For a given parameter set $\theta_1 = \{R_*, \mathbf{a}_*, \sigma_*^2\}$, two large sets of statistically independent random SCM pairs (realizations of $\mathbf{Y}$) were generated according to the statistical model given in section 2[1]. The first set simulates the of SCM pairs measured under H_0 where $\theta_0 = \{R_*\}$, and the second set corresponds to H_1 with θ_1. The test statistics of the various detectors, which are given in (7), (9), (28), (30), (32), were computed for the simulated SCM pairs[2]. Using the simulated test statistics, the P_d of the tested detectors was estimated as a function of the P_{fa}, for the simulated parameter set. This process was repeated to obtain estimations of the receiver operating characteristic (ROC) for different SBR values and transient source locations, with fixed BCM.

The important simulation parameters are: Random array with $q = 60$, maximum baseline of about 60 wavelengths, integrating $N = 5 \cdot 10^4$ vector samples for each SCM, integration interval of 1 second. BCM is composed of the 50 brightest stationary celestial sources taken from [6] + uniform uncorrelated receiver noise 13dB below the power of the brightest star. Transient source was positioned in one of 9 equally spaced locations in the sky, simulated SBR values ranged from -25dB to 7dB.

The simulation results are summarized in Figure 1. The P_d depicted in the graph is the lowest out of all the P_d values that were measured in the various transient locations when $P_{fa} = 10^{-4}$. It should be noted that the only detector whose performance was transient position dependent was the DI subtractor. It is evident from the simulation results that the detectors proposed in this paper, outperformed the DI subtractor significantly. Using the clairvoyant unrealizable bound we can see that for high P_d our detector is at most 1.5dB away from the optimal performance.

In practice, the MVDR ratio detector may be preferred since it requires less matrix multiplications for each matrix pair.

7. CONCLUDING REMARKS

In this paper we proposed two new detectors detecting radio astronomical transient signals. We showed that these detectors outperform the currently used detectors for this problem. We also provided asymptotic results for the large N distribution of the test statistics.

[1] The simulation is more realistic than the analytical model in the sense that differences in stationary source formation between the two sampling instances due to earth rotation are taken into consideration.

[2] To obtain a fair comparison, we used a variation of the DI difference detector that takes the DI image of $(\hat{R}_2 - \hat{R}_1)$ as input.

8. REFERENCES

[1] T. W. Anderson. Asymptotic theory for principal component analysis. *The Annals of Mathematical Statistics*, 34(1):122–148, 1963.

[2] T.W. Anderson. *An Introduction to Multivariate Statistical Analysis*. Wiley Series in Probability and Statistics. Wiley, 2003.

[3] Francesco Bandiera, Olivier Besson, Danilo Orlando, Giuseppe Ricci, and Louis L Scharf. GLRT-based direction detectors in homogeneous noise and subspace interference. *IEEE Transactions on Signal Processing*, 55(6):2386–2394, 2007.

[4] Jack Capon. High-resolution frequency-wavenumber spectrum analysis. *Proceedings of the IEEE*, 57(8):1408–1418, 1969.

[5] Cullum and Willoughby. *Lanczos Algorithms for Large Symmetric Eigenvalue Computations Vol. I Theory*. Birkhauser Basel, 1985.

[6] D.O. Edge, J.R. Shakeshaft, McAdam, W. B., J. E. Baldwin, and S. Archer. A survey of radio sources at a frequency of 159 mc/s. *Mem. R. Astron. Soc.*, 68:37–60, 1959.

[7] Gene H. Golub and Henk A. van der Vorst. Eigenvalue computation in the 20th century. *Journal of Computational and Applied Mathematics*, 123(1):35 – 65, 2000. Numerical Analysis 2000. Vol. III: Linear Algebra.

[8] R. Heimann, A. Leshem, E. Zehavi, and A. J. Weiss. Non-asymptotic performance bounds of eigenvalue based detection of signals in non-Gaussian noise. In *2016 IEEE International Conference on Acoustics, Speech and Signal Processing (ICASSP)*, pages 2936–2940, March 2016.

[9] Roger A Horn and Charles R Johnson. Matrix analysis cambridge university press. *New York*, 1985.

[10] Iain M. Johnstone. On the distribution of the largest eigenvalue in principal components analysis. *The Annals of Statistics*, 29(2):295–327, 2001.

[11] Iain M Johnstone. High dimensional statistical inference and random matrices. *arXiv preprint math/0611589*, 2006.

[12] S.M. Kay. *Fundamentals of Statistical Signal Processing: Detection theory*. Prentice Hall Signal Processing Series. Prentice-Hall PTR, 1998.

[13] S. Kraut, L. L. Scharf, and L. T. McWhorter. Adaptive subspace detectors. *IEEE Transactions on Signal Processing*, 49(1):1–16, Jan 2001.

[14] A. Leshem and A. J. van der Veen. Radio-astronomical imaging in the presence of strong radio interference. *IEEE Transactions on Information Theory*, 46(5):1730–1747, Aug 2000.

[15] Amir Leshem and A-J Van der Veen. Multichannel detection and spatial signature estimation with uncalibrated receivers. In *Statistical Signal Processing, 2001. Proceedings of the 11th IEEE Signal Processing Workshop on*, pages 190–193. IEEE, 2001.

[16] Amir Leshem and A-J Van der Veen. Multichannel detection of gaussian signals with uncalibrated receivers. *IEEE Signal Processing Letters*, 8(4):120–122, 2001.

[17] D. R. Lorimer, M. Bailes, M. A. McLaughlin, D. J. Narkevic, and F. Crawford. A bright millisecond radio burst of extragalactic origin. *Science*, 318(5851):777–780, 2007.

[18] R. Morganti. Synergy with new radio facilities: From LOFAR to SKA. *Astronomische Nachrichten*, 338(2-3):165–171, 2017.

[19] Petroff. FRB catalogue, 2016.

[20] B. W. Stappers and et al. Observing pulsars and fast transients with LOFAR. *A&A*, 530:A80, 2011.

[21] Stewart and et al. LOFAR MSSS: detection of a low-frequency radio transient in 400h of monitoring of the north celestial pole. *Monthly Notices of the Royal Astronomical Society*, 456(3):2321–2342, 2016.

[22] John Swinbank et al. A transient detection and monitoring pipeline for LOFAR. *proceedings of science*, 2007.